Dryout Heat Flux (DHF) Experiments of Debris Bed using a Hydrogen Evolving Method

Je-Young Moon and Bum-Jin Chung*
Department of Nuclear Engineering, Kyung Hee University
#1732 Deogyeong-daero, Giheung-gu, Yongin-si, Gyeonggi-do, 17104, Korea
**Corresponding author*: bjchung@khu.ac.kr

1. Introduction

An ex-vessel scenario of molten corium after reactor pressure vessel (RPV) failure is depicted by jet break-up, droplet solidification and debris bed settling in sequence (Fig. 1). The relocated debris bed may lead the molten corium-concrete interaction (MCCI) [1-6]. In order to avoid the MCCI, it is important to evaluate the coolability of the debris beds. Boiling of water removes the decay heat of debris bed. Thus, the dryout heat flux (DHF) is considered as the maximum heat removal rate of debris bed [7-13]. It is essential to investigate the influence of parameters (particle diameter, bed height, flooding condition, etc.) on the coolability of debris beds.

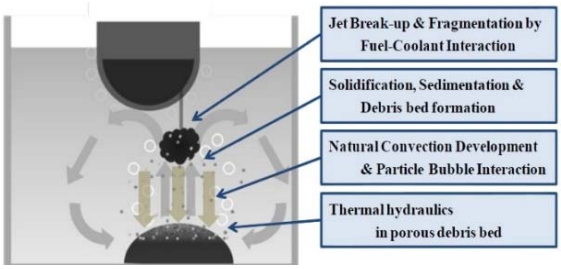

Fig. 1. A development process of corium debris bed in the flooded cavity pool [6].

We measured the dryout heat fluxes (DHF) of debris beds by a non-heating experimental method. The vaporization occurred in debris bed was simulated by the hydrogen gas generated at the cathode due to the applied electric potential in the aqueous solution of H_2SO_4. The copper or stainless steel cathode acted as heated particles. For the bottom flooding condition, the particle diameters and bed heights were 3 mm to 6 mm and 20 mm to 60 mm, respectively. Also, in order to analyze the characteristics of hydrogen bubbles, we performed the visualization using high speed camera.

2. Theoretical background

The existing studies reported that the coolability of debris bed is affected by the particle diameter, bed height, system pressure, flooding and coolant conditions, etc. Particularly, the DHF depends on the particle diameter, bed height and flooding condition.

The effects of particle diameter and bed height with top flooding condition were experimentally studied by Barleon *et al.* [8]. The particle diameter and bed height were varied 0.06 to 16 mm and 6 to 40 cm, respectively. The water or Freon-113 was used as the coolant. They reported the DHF increased with the particle diameter and decreased with the bed height regardless of coolant [14].

Hofmann [15] also performed the DHF experiments for top flooding and bottom flooding condition. The bed height varied up to 0.5 m and consisted of 3 mm stainless steel particles. The coolant was the water. The DHF for bottom flooding condition was more than twice as high as that from top flooding condition. The similar results for the flooding condition were reported by Atkhen and Berthoud [3], Rashid *et al.* [11], Squarer and Peoples [18], and Kulkarni *et al.* [19].

Afterward, Hofmann [16] confirmed the influence of the particle diameter and bed height on the DHF for the top flooding condition. The uniform beds consisted of stainless steel balls of 1 and 3 mm in diameter up to 100 cm height. They mentioned that the DHF decreased with increasing bed height. Dhir and Catton [17] also reported the similar result. Yamano *et al.* [1], Kim *et al.* [6], Bang and Kim [12], Hofmann [16], Squarer and Peoples [18] also confirmed the dryout heat density was improved by the particle diameter.

Even though there have been considerable studies on the DHF of the debris bed either experimentally or theoretically, the range of parameters (particle diameter, bed height, porosity, etc.) was scattered due to uncertainty about the formation and settling of debris bed. Thus, it is difficult to compare the results of the existing studies.

3. Experimental setup

3.1 Non-heated hydrogen evolving method

For a single phase, heat and mass transfer systems are proved to be analogous [20] and the experimental method using a copper sulfate-sulfuric acid ($CuSO_4$-H_2SO_4) electroplating system based on the analogy concept has been used for heat transfer studies [21-25].

In this system, we used the evolution of hydrogen gas when the applied electric potential between anode and cathode increases to simulate the bubbles. When the electric potential is applied between the cathodes and anode, all the cathode particles have the same electric potential, which means that a uniformly heating condition can be easily simulated.

We hypothesized that hydraulic behavior of hydrogen gas over the arbitrary solid surface will be similar under the identical gaseous volume generation rate (η). Especially as the DHF phenomena will be a complex combination of the gas generation and removing by hydrodynamics, a successful application of the idea to the gap CHF(Critical Heat Flux) by Ohk *et al.* [26] can

be extended to the DHF phenomena. Thus, the DHF can be calculated with Eq. (1) introducing the gas generation rate (η).

$$q_{DHF} = \eta h_{lg} \rho_g \tag{1}$$

The hydrogen generation rate (η) is determined by the electric current, charges for hydrogen reduction and Avogadro number (Eq. (2)).

$$\eta = V_m \left(\frac{T}{273.15} \right) \left(\frac{I}{neN_A} \right) \tag{2}$$

3.2 Experimental apparatus

Figure 2 shows the electric circuit of the experimental apparatus consisted of a polycarbonate pipe containing the cathode particles and anode, a power supply and a data acquisition (DAQ) system. The inner diameter and length of cathode part pipe are 46 mm and 815 mm. respectively. The diameter of copper and stainless steel particles is 3 to 6 mm. Also, the bed height is ranged from 20 to 60 mm. The test section is filled with the sulfuric acid solution (H_2SO_4) of 1.5 M. For the bottom flooding condition, the top and bottom of bed were open and the copper cathode bed were rested on a permeable support grid. The porosities of beds are 0.374 to 0.490 for all cases. The copper anode of 35 mm × 35 mm × 100 mm are placed at the lower part of the pipe to supply the electric charges.

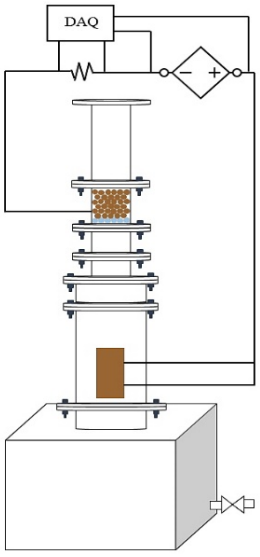

Fig. 2. The electric circuit of experimental apparatus.

Figure 3 presents the front view of test section for visualization. The copper balls of 4 mm in diameter acted as the cathode particles. In order to observe the distinct behavior of hydrogen bubbles, the square duct of polycarbonate is filled with copper bed of body-centered cubic (BCC) structure and aqueous solution of the sulfuric acid (H_2SO_4).

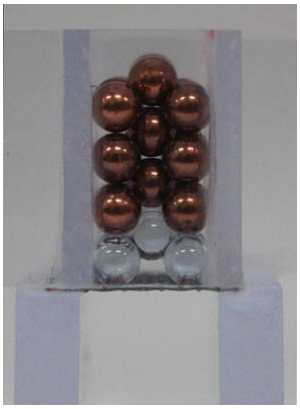

Fig. 3. Front view of test section for visualization.

4. Results and discussion

Figure 4 indicates the measured currents depending on the applied potentials. A step increase of the electric potential is made until a sudden drops of the current were observed. For high power, the pressure developed by the generated hydrogen gas retards the inflow of H_2SO_4 solution into the copper bed. The flow of the electric current is blocked by the hydrogen gas. It is similar to the dryout mechanism of heat transfer system. For other cases, the same mechanism was observed.

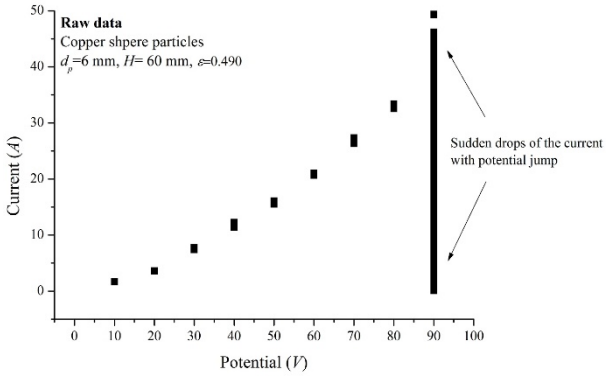

Fig. 4. Potential and current values reaching the dryout.

Figure 5 presents the measured current and potential at the stabilized conditions. As a result, the calculated DHF by using Eq. (1) and (2) was 2.98 kW/m^2. Figures 6 and 7 show the DHF depending on the bed height and particle diameter for the bottom flooding condition. The DHF decreases with the bed height regardless of the cathode materials and increases with the particle diameter. This tendency of measured DHF is similar to that of existing heat transfer studies [3, 8, 12, 15-18]. However, the absolute values were quite different. This discrepancy seems to be due to the differences in the bubble characteristics influencing the dryout mechanism. Thus, we performed the visualization experiments to investigate the characteristics of hydrogen bubble.

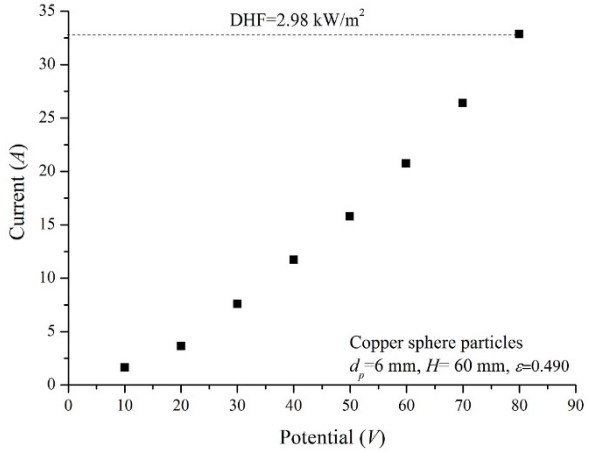

Fig. 5. Average potential and current values at equilibrium state reaching the dryout for the copper beds of H=60 mm.

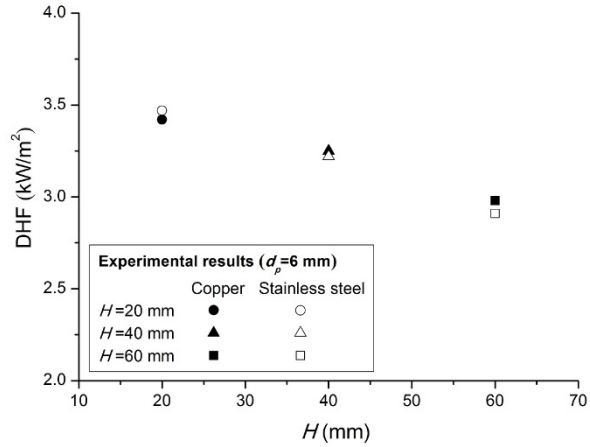

Fig. 6. Dryout heat flux according to the bed height of copper and stainless steel beds of d_p=6 mm.

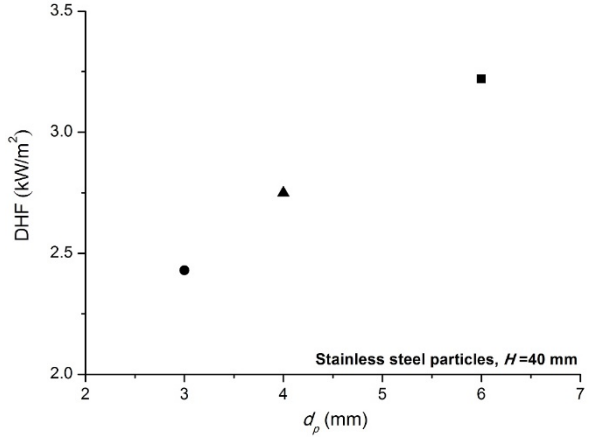

Fig. 7. Dryout heat flux depending on the particle diameter.

In the present electrochemical system, the diameter of hydrogen bubbles is about twenty times smaller than that of the boiling system as shown in Fig. 8. Also, many nucleation sites were observed. Thus, a plausible explanation for the discrepancy of the DHF values is that the electric resistance of cathode particles had increased as the smaller hydrogen bubble and too many nucleation site caused the decrease of cathode surface.

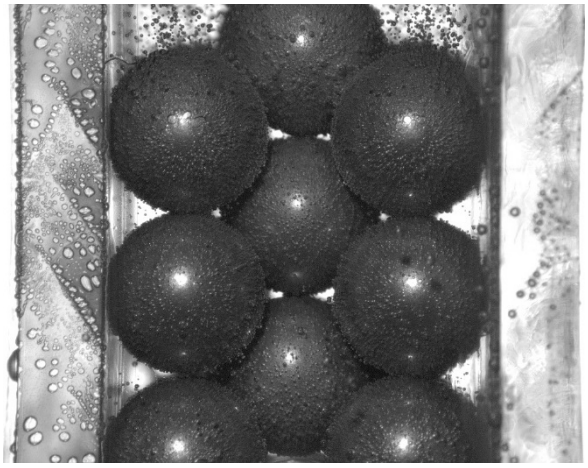

(a) Behavior of hydrogen bubble at 1 V

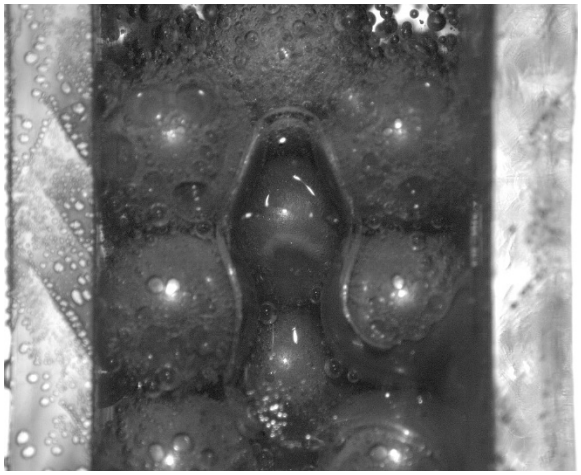

(b) Behavior of hydrogen bubble at 5 V

Fig. 8. The behavior of hydrogen bubble with potential.

5. Conclusions

The dryout heat fluxes (DHF) were measured by the non-heated hydrogen evolving method. This method of DHF measurement simulates the uniform self-heating condition of debris bed.

The DHF can be directly calculated by the measured electric current from the present study. The DHF was increased by the increase of the particle diameter and the decrease of the bed height regardless of the cathode materials. This tendency for the DHF is similar to that of existing studies. However, the measured DHF values had large discrepancy.

Visualization experiments showed clear difference between hydrogen bubbles and vapor ones in terms of bubble diameter, nucleation site density, etc. Thus, the discrepancy is natural due to the bubble characteristics influencing the boiling mechanism. Also, the bottom flooding condition wasn't fully simulated because the captured hydrogen bubbles were observed at the underneath of the permeable support grid. As the captured bubbles obstructed the inflow of the sulfuric acid solution, the dryout condition was reached early.

Thus, we would develop the correction factor (bubble diameter, bubble volume, etc.) to establish the similarity between heat and mass transfer system. An idea is to incorporate the difference in bubble diameter for the estimation of the DHF. Another idea is to setup a relative relationship among different thermal boundary conditions instead of pursuing the estimation of the absolute DHF values.

ACKNOWLEDGEMENT

This study was sponsored by the Ministry of Science and ICT (MSIT) and was supported by Nuclear Research & Development program grant funded by the National Research Foundation (NRF) (Grant code: 2017M2A8A4056304).

REFERENCES

[1] N. Yamano *et al.*, TECHNICAL NOTE ON EX-VESSEL CORE MELT DEBRIS COOLABILITY AND STEAM EXPLOSIONS, NEA/CSNI/R(96)24, 1996.
[2] Y. Maruyama *et al.*, RECENT RESULTS OF MCCI STUDIES IN COTELS PROJECT, Third Korea-Japan Symposium on Nuclear Thermal Hydraulics and Safety (NTHAS3), Gyeongju, Korea, Oct. 13-16, 2002.
[3] K. Atkhen, G. Berthoud, SILFIDE experiment: Coolability in a volumetrically heated debris bed, Nuclear Engineering and Design, 236, 2126-2134, 2006.
[4] H.J. Allelein, M. Bürger, Considerations on ex-vessel corium behavior: Scenarios, MCCI and coolability, Nuclear Engineering and Design, 236, 2220-2236, 2006
[5] M.T. Farmer *et al.*, CORIUM COOLABILITY UNDER EX-VESSEL ACCIDENT CONDITIONS FOR LWRs, Nuclear Engineering and Technology, 41(5), 575-602, 2009.
[6] E.H. Kim *et al.*, Experimental Study on the Ex-Vessel Corium Debris Bed Development under Two-Phase Natural Convection Flows in Flooded Cavity Pool, The 7th European Review Meeting on Severe Accident Research (ERMSAR-2015), Marseille, France, Mar. 24-26, 2015.
[7] K. Hu, T.G. Theofanous, ON THE MEASUREMENT AND MECHANISM OF DRYOUT IN VOLUMETRICALLY HEATED COARSE PARTICLE BEDS, International Journal of Multiphase Flow, 17(4), 519-532, 1991.
[8] L. Barleon *et al.*, COOLING OF DEBRIS BEDS, Nuclear Technology, 65, 67-86, 1984.
[9] P. Schäfer *et al.*, Basic investigations on debris cooling, Nuclear Engineering and Design, 236, 2104-2116, 2006.
[10] E. Takasuo, An experimental study of the coolability of debris beds with geometry variations, Annals of Nuclear Energy, 92, 251-261, 2016.
[11] M. Rashid *et al.*, Experimental results on the coolability of a debris bed with multidimensional cooling effects, Nuclear Engineering and Design, 241, 4537-4543, 2011.
[12] K.H. Bang, J.M. Kim, ENHANCEMENT OF DRYOUT HEAT FLUX IN A DEBRIS BED BY FORCED COOLANT FLOW FROM BELOW, Nuclear Engineering and Technology, 42(3), 297-304, 2010.
[13] G. Repetto *et al.*, Investigation of Multidimensional Effects during Debris Cooling, The 5th European Review Meeting on Severe Accident Research (ERMSAR-2012), Cologne, Germany, mar. 21-23, 2012.
[14] R.J. Lipinski, A model for Boiling and Dryout in Particle beds, NUREG/CR-2646, 1982.
[15] G. Hofmann, ON THE LOCATION AND MECHANISMS OF DRYOUT IN TOP-FED AND BOTTOM-FED PARTICULATE BEDS, Nuclear Technology, 65, 36-45, 1984.
[16] G. Hofmann, DRYOUT IN VERY DEEP PARTICULATE BEDS, Nuclear Engineering and Design, 99, 177-185, 1987.
[17] V.K. Dhir, I. Catton, Dryout Heat Fluxes in Very Deep Debris Beds, Transactions of the American Nuclear Society, 35, 360-361, 1980.
[18] D. Squarer, J.A. Peoples, Dryout during Inductively-Heated Bed With and Without Forced Flow, Transactions of the American Nuclear Society, 34, 535-537, 1980.
[19] P.P. Kulkarni *et al.*, Experimental investigation of coolability behavior of irregularly shaped particulate debris bed, Nuclear Engineering and Design, 240, 3067-3077, 2010.
[20] A. Bejan, Convection Heat Transfer, fourth ed. Wiley & Sons, New Jersey, 2003.
[21] E.J. Fenech, C.W. Tobias, Mass transfer by free convection at horizontal electrodes, Electrochimica Acta, 2, 311-325, 1960.
[22] J.R. Selman, C.W. Tobias, Mass-transfer measurement by the limiting-current technique, Advance in Chemical Engineering, 10, 211-318, 1978.
[23] C.W. Tobias, R.G. Hickman, Ionic mass transfer by combined free and forced convection, Zeitschrift für Physikalische Chemie-International Journal of Research in Physical Chemistry Chemical Physics, 229, 145-166, 1965.
[24] S.H. Ko *et al.*, Applications of electroplating method for heat transfer studies using analogy concept, Nuclear Engineering and Technology, 38, 251-258, 2006.
[25] H.K. Park, B.J. Chung, Mass Transfer Experiments for the Heat Load during In-Vessel Retention of Core Melt, Nuclear Engineering and Technology, 48, 906-914, 2016.
[26] S.M. Ohk *et al.*, CHF Experiments on the influence of inclination and gap size, International Journal of Heat and Mass Transfer, 132, 929-938, 2019.